Large-Scale Synthesis of Six-Nanometer-Wide ZnO Nanobelts

Xudong Wang, Yong Ding, Christopher J. Summers, and Zhong Lin Wang*

School of Materials Science and Engineering, Georgia Institute of Technology, Atlanta, Georgia 30332-0245

Received: April 6, 2004; In Final Form: April 29, 2004

Using a thin film of metallic tin as catalyst, ultrasmall single-crystalline zinc oxide nanobelts have been synthesized in large quantity using a simple solid−vapor technique. The nanobelts have an average width of 5.5 nm and a narrow size distribution of ±1.5 nm. The nanobelts grew along the [0001] direction, with $(2\bar{1}\bar{1}0)$ top/bottom surfaces and $(01\bar{1}0)$ side surfaces. Photoluminescence measurement showed a blue shift in the emission spectrum compared to that acquired from ZnO nanobelts of ∼200 nm in width. These ultrafine nanobelts should be good candidates for investigating size-induced electrical and optical properties of functional oxides.

Quasi-one-dimensional (1D) nanostructures,[1] such as nanobelts[2] and nanowires,[3] have recently attracted a lot of research interest due to their unique properties and wide range of applications. A wide range of techniques have been developed for the synthesis of 1D nanostructures, including solid−vapor deposition,[2−4] lithography,[4] laser ablation,[5] sol−gel,[6] and template-assisted methods;[7,8] and nanowires and nanobelts with sizes in the range of 10−100 nm have been synthesized. In general, it is believed that nanowires less than 10 nm will have novel and unique physical and chemical properties due to quantum confinement. Nanowires of a few nanometers in size have been synthesized for InP[9] and Si.[10]

Zinc oxide, a direct wide band gap (3.37 eV) semiconductor with a large excitation binding energy (60 meV), is one of the most important functional oxides, exhibiting near-UV emission, transparent conductivity, and piezoelectricity. Intensive research has been focused on fabricating 1D ZnO nanostructures and in correlating their morphology with their size-related optical and electrical properties.[11,12] Thermal evaporation is a highly effective technique for fabricating 1D ZnO nanostructures both in large quantities and at low cost, and gold,[10−13] copper,[14] and tin[15] have been successfully used as catalysts to direct the growth of 1D ZnO nanostructures by a vapor−liquid−solid (VLS) process. Due to the fact that solid−vapor phase synthesis typically occurs at high temperature, 700−1300 °C, the synthesis of small-size (<10 nm) ZnO nanobelts and nanobelts with large yield is cumbersome.

In this paper, we report a novel but simple technique for the synthesis of ultrasmall single-crystalline zinc oxide nanobelts in large quantity by solid−vapor deposition. The nanobelts have an average width of 5.5 nm and a narrow size distribution of ±1.5 nm, and should be good candidates for investigating size-induced electrical and optical properties of functional oxides.

The ultrasmall nanobelts were synthesized by a solid−vapor phase process using a novel catalyst. In the experimental process, a silicon substrate was first cleaned by a 2:1 mixture (by volume) of H_2SO_4 (98%) and H_2O_2. However, instead of using dispersive nanoparticles as the catalyst for size-controlled seeding growth, a uniform thin film (∼10 nm) of tin was coated on the silicon substrate. A thermal evaporator with a quartz crystal thickness monitor was used to reproducibly obtain the exact film thickness for the tin layer. For nanobelt growth, equal moles of ZnO powder and graphite powder were grounded together and loaded into an alumina boat. The source materials were located at the center of an alumina tube and the substrate was placed downstream (15−20 cm) from the center, where the local growth temperature is about 250−300 °C. A horizontal tube furnace was used to heat the tube to 850−860 °C at a rate of 50 °C/min, and the temperature was held for 15 min under a pressure of 250−300 mbar with a constant argon flow at 20 sccm. The structural properties of the products were characterized by scanning electron microscopy (SEM) (LEO 1530 FEG at 10 kV), transmission electron microscopy (TEM) (JEOL 100 °C at 100 kV), and high-resolution TEM (JEOL 4000 EX at 200 kV), and the optical properties were measured by a UV photoluminescence (PL) system at room temperature using a Xe lamp with an excitation wavelength of 330 nm.

The morphology of the ZnO nanobelts was first examined by SEM. Figure 1a shows a low magnification SEM image of the ultra small ZnO nanobelts obtained from growth on a silicon wafer coated with a 10 nm tin layer. Because the mutual solubility of silicon and tin is limited, during the initial heating process, the thin tin layer agglomerates into balls due to surface tension. The white balls in Figure 1b then become the tin catalyst for nanobelt growth. The lengths of the nanobelts are typically a few micrometers and exhibit a uniform size distribution. The ZnO nanobelts extend out from the tin balls and cover the whole substrate with a reasonable yield, which can be seen more clearly in a higher-magnification SEM image given in Figure 1c.

Unlike other reported metal-seeded VLS growth techniques, which normally have a metal ball at the tip of the ZnO nanowires,[15] these nanobelts have clean tips. Thus we believe the active growth surface is at the root of the nanobelt due to the large size of the catalyst, and this growth still occurs by the VLS process. The schematic growth processes are illustrated in Figure 2. Since tin has a very low melting point (232 °C), it is molten before the ZnO vapor is formed in the reaction tube (Figure 2a and b), even though the substrate deposition temperature is lower than that of the ZnO source. Once the temperature becomes high enough to produce Zn/ZnO vapor, the surface of the liquid tin immediately supersaturates, thus, ZnO precipitates out at these nucleation seeds. By keeping a

* Corresponding author. E-mail: zhong.wang@mse.gatech.edu.

10.1021/jp048482e CCC: $27.50
Published on Web 05/26/2004

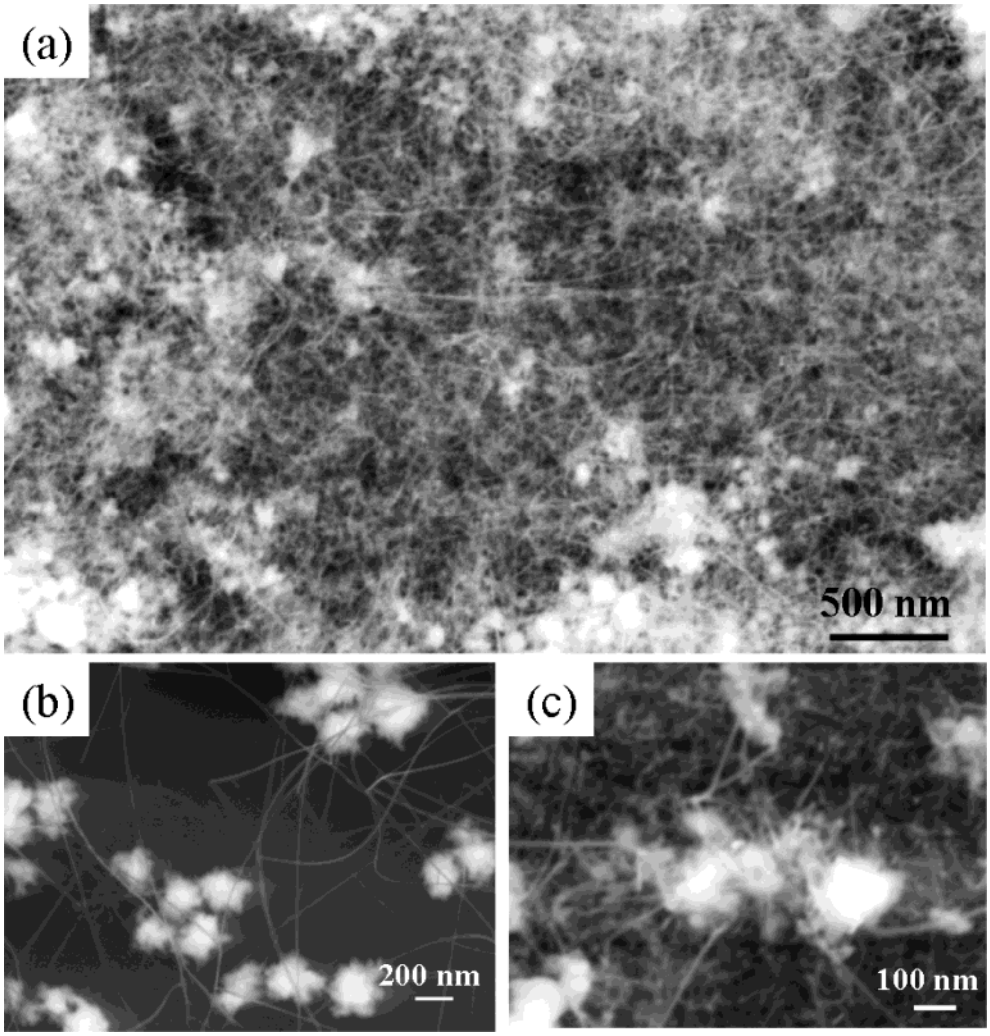

Figure 1. SEM images of ultrathin ZnO nanobelts grown on tin-coated silicon substrate. (a) Low-magnification image, (b) higher-magnification image showing tin catalysts, (c) higher-magnification image showing ZnO nanobelts extended out from tin balls.

reasonable vapor pressure of ZnO in the furnace, the ZnO nanobelts continue to grow from the tin surface (Figure 2c), i.e., push up from the supersaturated growth surface. Figure 2d shows the TEM image of the ZnO nanobelts grown on top of the tin surface. Therefore, the effective catalyst for growth is the large tin particles and it is not necessary to pre-synthesize catalyst nanoparticles to control the size of the nanobelts. This is in contrast to conventional VLS growth, where a pretreatment of catalyst is traditionally necessary for size determination.[16] Thus, this method provides a much simpler way to fabricate ultrathin ZnO nanobelts at lower cost and at large quantity and can be extended to a variety of inorganic materials.

By measuring over 120 nanobelts from randomly recorded TEM images, the average diameter of the nanobelts was determined to be 5.5 nm with a standard deviation of ± 1.5 nm. As shown in Figure 3e, most nanobelts are in the range of $4-7$ nm, indicating very good size uniformity. A sample exhibiting this size uniformity and distribution is presented by the TEM image shown in Figure 3a.

Figure 3b shows an electron diffraction pattern recorded from a relatively large ZnO nanobelt shown in Figure 3c. The diffraction pattern corresponds to the $[2\bar{1}\bar{1}0]$ zone axis of wurtzite ZnO, and displays the fastest growth direction of ZnO nanobelts as being [0001]. The contrast in Figures 3c and 3d is due to bending-induced strain,[17] and the image indicates the equal projected thickness of the nanobelt. The top surfaces of the nanobelts are $(2\bar{1}\bar{1}0)$ and the side surfaces are $(01\bar{1}0)$.

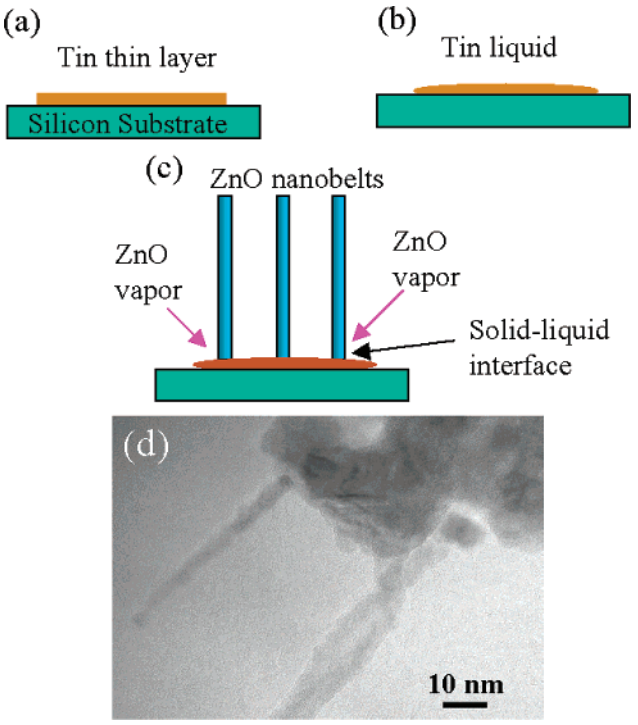

Figure 2. (a−c) Schematic steps of the growth of ZnO nanobelts on tin catalyst. (d) ZnO nanobelts growing on the top of tin.

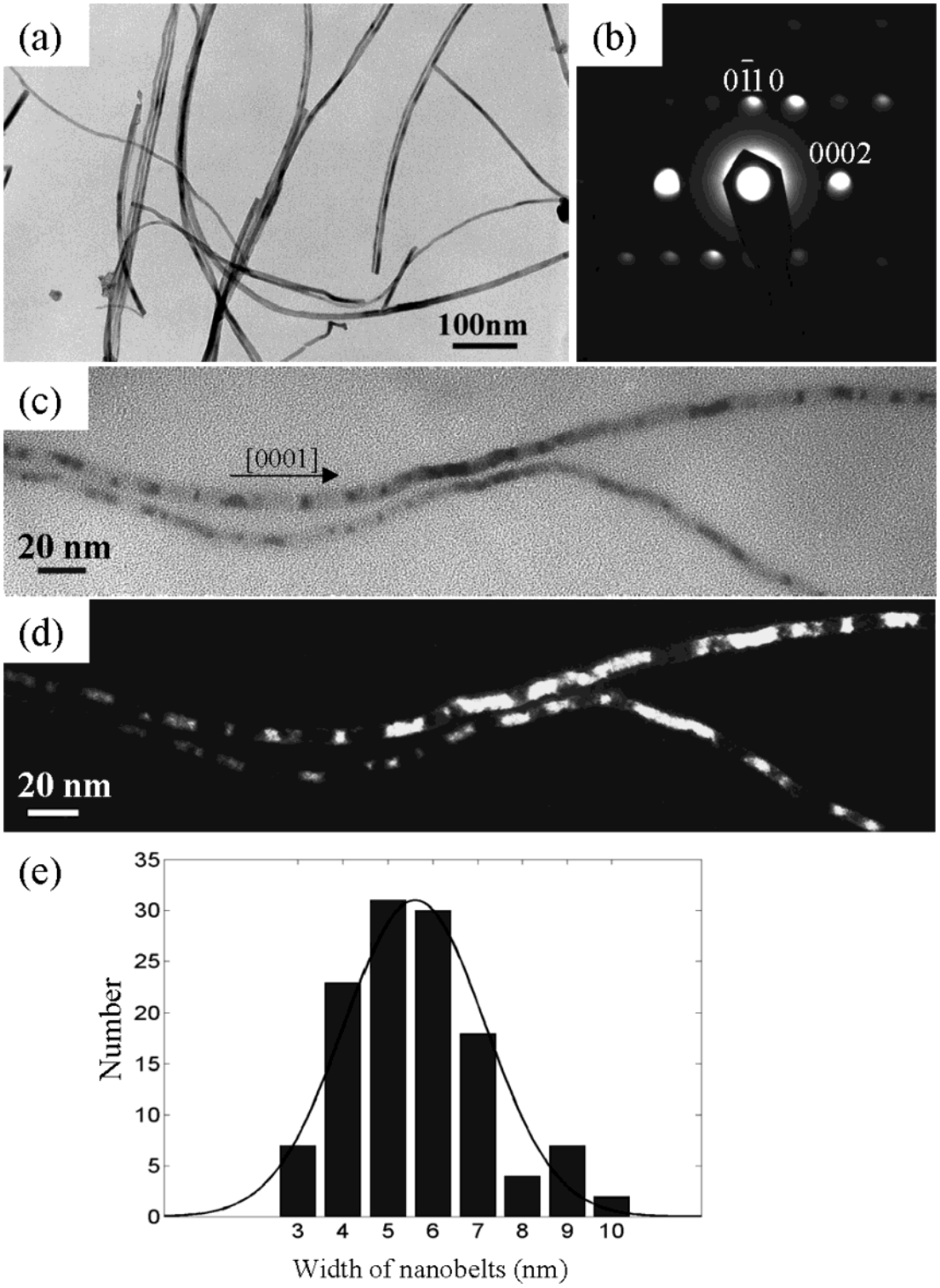

Figure 3. (a) Low-magnification TEM image showing the size uniformity of ZnO nanobelts. (b−d) Diffraction pattern, bright field image, and dark field image of ZnO nanobelts that have a belt-like morphology. (e) Size distribution of as-synthesized ZnO nanobelts.

High-resolution TEM has been employed to study the strain release mechanism in ZnO nanobelts (Figure 4). All of the nanobelts display a single-crystalline structure with the (0001) fringes of spacing 5.1 Å. Due to the root-growth process, the bending of the nanobelts introduces a large local strain. This is demonstrated by the fact that a nanobelt 10 nm in width is straight (Figure 4a), while a thin nanobelt 5 nm in width shows a curly shape (Figure 4b). The strain in the thicker nanobelt is released by creating stacking faults perpendicular to the growth direction of the nanobelts (Figure 4c). For the ∼5 nm nanobelt, besides stacking faults, distortion in the orientation of the (0001) atomic planes (Figure 4d) and edge dislocations (Figure 4e) are introduced to accommodate the local deformation. This is a rather surprising effect because it is normally believed that no dislocation is present in nanowires/nanobelts, particularly when their sizes are small. The interplanar distance can be expanded to ∼5.4 Å at the exterior arc and compressed to ∼4.8 Å at the inner arc to accommodate the local strain. This is possible for narrow nanobelts. The creation of edge dislocations in oxide nanobelts is rare.

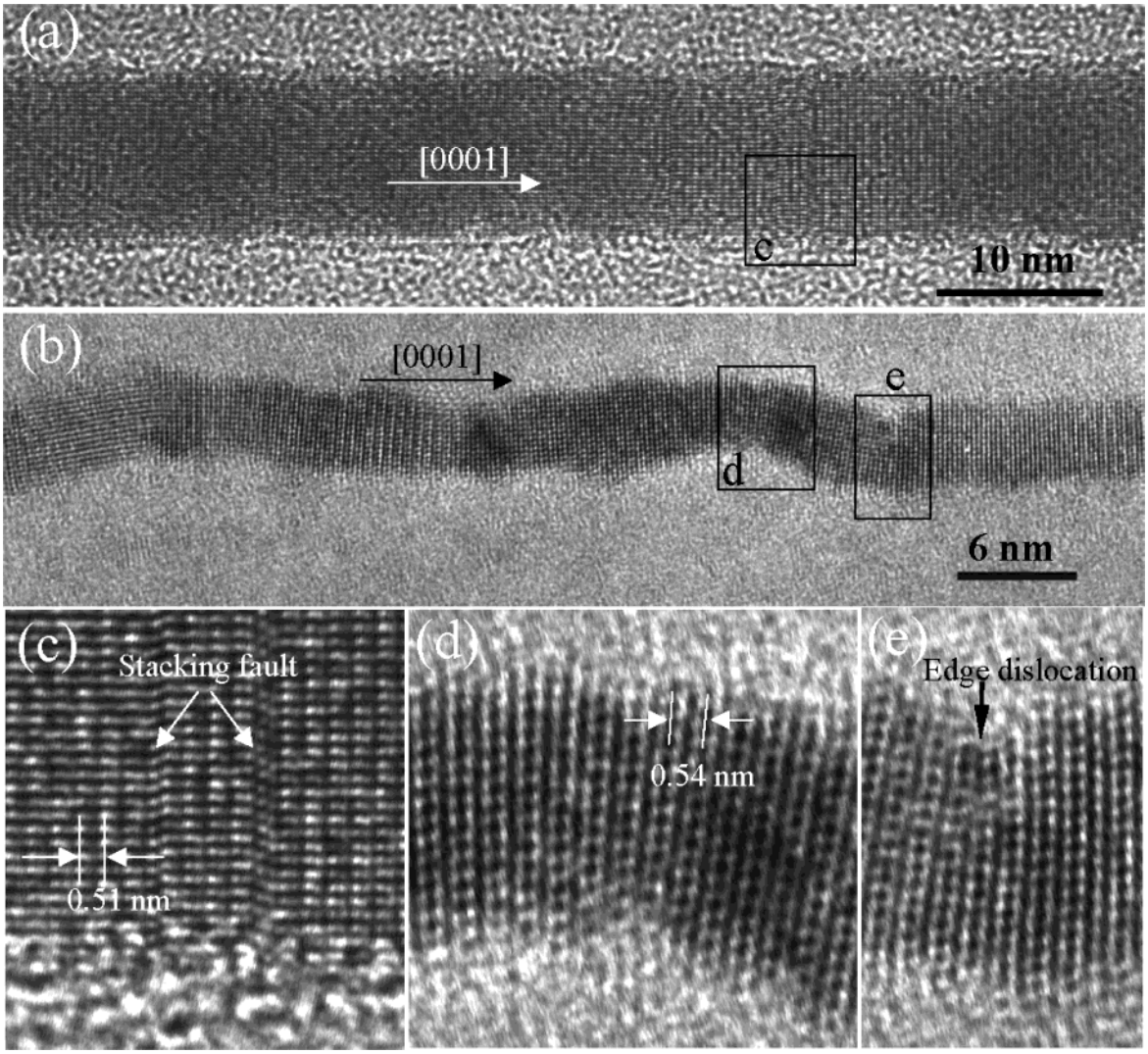

Figure 4. High-resolution TEM images of (a) 10 nm-wide and (b) 5 nm-wide ZnO nanobelts. (c−e) The enlarged images from areas c, d, and e marked in (a) and (b), respectively, showing strain-induced change in interplanar distance and an edge dislocation in the nanobelt.

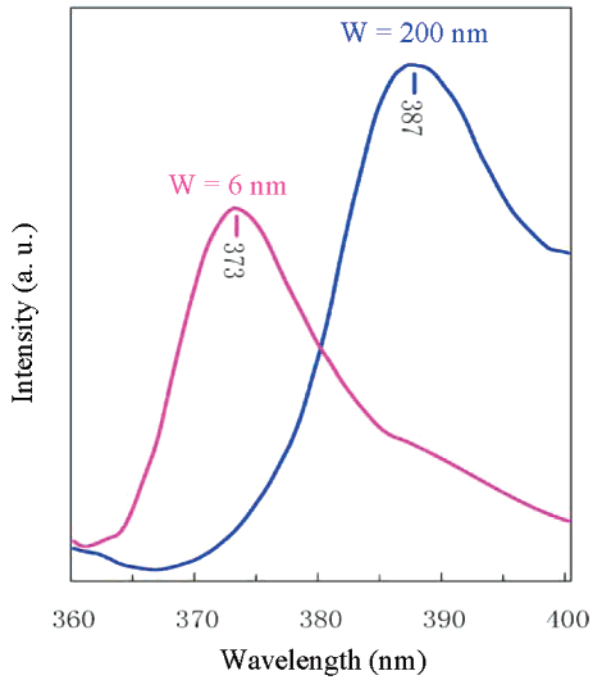

Figure 5. Photoluminescence spectra acquired from the ~200-nm wide ZnO nanobelts and the 6 nm-wide ZnO nanobelts.

To examine the size-dependent property of the ultra-narrow ZnO nanobelts, photoluminescence (PL) measurements were performed at room temperature using a Xe lamp with an excitation wavelength of 330 nm. Figure 5 compares the PL spectra recorded from the ZnO nanobelts synthesized previously that have an average width of ~200 nm and the PL from the ultrathin ZnO nanobelts with an average width of 5.5 nm. The 387 nm peak corresponds to a 3.2 eV spontaneous emission of the normal ZnO nanobelts, as reported previously.[8] This emission lies at an energy considerably below that of the band gap (3.37 eV) of ZnO. The ultrathin ZnO nanobelts exhibit a near band edge emission at 373 nm (3.32 eV), which was measured under identical experimental conditions as for the larger nanobelts.

Single-crystalline, ultrathin ZnO nanobelts have been synthesized using a solid−vapor deposition method. The deposition was performed on silicon substrates coated with a thin layer of tin. The average width of the nanobelts was 5.5 nm with a narrow size distribution of 1.5 nm. This self-nucleation process provides a novel but simple way to fabricate 1D nanostructures in large quantity without using pre-synthesized catalyst nanoparticles for size confinement. A 120 meV blue shift was observed in the photoluminescence spectra of the ZnO nanobelts. Ultrafine nanobelts are expected to have interesting electrical and optical properties.

Acknowledgment. We acknowledge financial support from the US NSF Grant DMR-9733160 and the MURI program from ARO (DAAD19-01-1-0603), and the Georgia Tech Electron Microscopy Center for providing the research facility. We thank Dr. Brent Wagner for his help in tin coating.

References and Notes

(1) Wang, Z. L. *Nanowires and Nanobelts*, Vol. I: *Metal and Semiconductor Nanowires*, and Vol. II: *Nanowire and Nanobelt of Functional Oxide*; Kluwer Academic Publisher: New York, 2003.

(2) Pan, Z. W.; Dai, Z. R.; Wang, Z. L. *Science* **2001**, *291*, 1947.

(3) Hu, J.; Odom T. W.; Lieber, C. M. *Acc. Chem. Res.* **1999**, *32*, 435.

(4) Ma, C.; Berta, Y.; Wang, Z. L. *Solid State Commun*. **2004**, *129*, 681.

(5) Duan, X.; Lieber, C. M. *J. Am. Chem. Soc.* **2000**, *122*, 188.

(6) Krumeich, F.; Muhr, H. J.; Niederberger, M.; Bieri, F.; Schnyder, B.; Nesper, R. *J. Am. Chem. Soc.* **1999**, *121*, 8324.

(7) Liu, C.; Zapien, J. A.; Yao, Y.; Meng, X.; Lee, C. S.; Fan, S.; Lifshitz, Y.; Lee, S. T. *Adv. Mater.* **2003**, *15*, 838.

(8) Wang, X. D.; Gao, P.; Li, J.; Summers, C. J.; Wang, Z. L. *Adv. Mater.* **2002**, *14*, 1732.

(9) Gudiksen, M. S.; Wang, J.; Lieber, C. M. *J. Phys. Chem. B* **2001**, *105*, 4062.

(10) Ma, D. D. D.; Lee, C. S.; Au, F. C. K.; Tong, S. Y.; Lee, S. T. *Science* **2003**, *299*, 1874.

(11) Huang, M. H.; Mao, S.; Feick, H.; Yan, H.; Wu, Y.; Kind, H.; Weber, E.; Russo, R.; Yang, P. *Science* **2001**, *292*, 1897.

(12) Zhao, Q. X.; Willander, M.; Morjan, R. R.; Hu, Q. H.; Campbell, E. E. B. *Appl. Phys. Lett.* **2003**, *83*, 165.

(13) Ng, H. T.; Chen, B.; Li, J.; Han, J.; Meyyappan, M.; Wu, J.; Li, S. X.; Haller, E. E. *Appl. Phys. Lett.* **2003**, *82*, 2023.

(14) Li, S. Y.; Lee, C. Y.; Tseng, T. Y. *J. Cryst. Growth* **2003**, *247*, 357.

(15) Gao, P. X.; Wang, Z. L. *J. Phys. Chem. B* **2002**, *106*, 12653.

(16) Cui, Y.; Lauhon, L. J.; Gudiksen, M. S.; Wang, J.; Lieber, C. M. *Appl. Phys. Lett.* **2001**, *78*, 2214.

(17) Wang, Z. L.; Kang, Z. C. *Functional and Smart Materials-Structure Evolution and Structure Analysis*; Plenum: New York, 1998.